Robust performance of self-scheduled LPV control of doubly-fed induction generator in wind energy conversion systems

Nguyen Tien, H.; Scherer, C. W.; Scherpen, J. M. A.

Published in:
2007 European Conference on Power Electronics and Applications, EPE

IMPORTANT NOTE: You are advised to consult the publisher's version (publisher's PDF) if you wish to cite from it. Please check the document version below.

Document Version
Publisher's PDF, also known as Version of record

Publication date:
2007

Citation for published version (APA):
Nguyen Tien, H., Scherer, C. W., & Scherpen, J. M. A. (2007). Robust performance of self-scheduled LPV control of doubly-fed induction generator in wind energy conversion systems. In *2007 European Conference on Power Electronics and Applications, EPE* University of Groningen, Research Institute of Technology and Management.

Robust performance of self-scheduled LPV control of doubly-fed induction generator in wind energy conversion systems

H. Nguyen Tien[1], C. W. Scherer[1], J. M. A. Scherpen[2]

[1] Delft Center for Systems and Control, Delft University of Technology, The Netherlands

[2] Faculty of Mathematics and Natural Sciences, University of Groningen, The Netherlands

Keywords

<<Robustness>>, <<Modelling>>, <<Simulation>>, <<Vector control>>, <<Wind energy>>.

Abstract

This paper describes the design of a self-scheduled current controller for doubly-fed induction generators in wind energy conversion systems (WECS). The design is based on viewing the mechanical angular speed as an uncertain yet online measurable parameter and on subsuming the problem into the framework of linear parameter-varying (LPV) controller synthesis. An LPV controller is then synthesized to guarantee a bound on the worst-case energy gain for all admissible trajectories of rotor speed in the operating range. Furthermore, this study investigates the robust performance of the LPV controller with respect to other bounded machine parameter variations and the impact of the stator voltage dips on the robustness of the control system. Two closed loop simulation models, one with a conventional control scheme and the other with an LPV control scheme, are developed for the control of the electrical torque and the power factor on the rotor side in order to compare the performance of the control systems. Some simulation results are given to demonstrate the performance and robustness of the control algorithm.

1 Introduction

Doubly fed induction machines (DFIMs) are recently considered to be an attractive solution for wind energy conversion systems (WECS) since they can be controlled efficiently in a wide speed-variable range. Suitable control strategies can be used to optimize the power converted from wind energy into electrical energy both from the stator and the rotor. Control actuation is performed at the rotor side through slip rings. This allows a reduction of the size of the power converter and, hence, of the cost of the overall system, especially at high-power levels.

In the regular configuration of variable speed wind turbines, the stator of DFIM is directly connected to the grid and the rotor is connected with two converters, one in the grid side, the so-called Grid Side Converter (GSC), and one in the rotor side, the so-called Rotor Side Converter (RSC), coupled by a DC-voltage link as shown in Figure 1.

1.1 Modelling and control of doubly-fed induction machine

In this paper, a dq reference frame that has the d axis coinciding with the grid voltage vector is adopted. In this reference frame, the DFIM equations can be written as

$$\dot{x}_r = A_{rc}(\omega)x_r + B_s v_s + B_r v_r \tag{1}$$
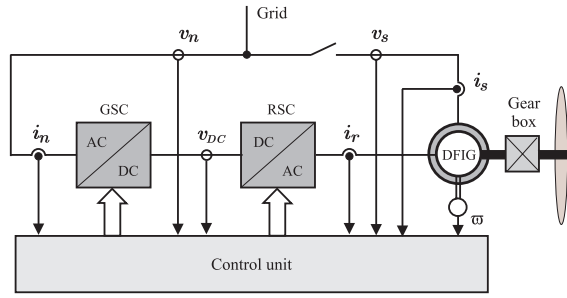
$$y_r = C_{rc}x_r \tag{2}$$

Figure 1: Variable speed wind turbine system

where $x_r = \begin{pmatrix} i_{rd} & i_{rq} & \Psi_{sd} & \Psi_{sq} \end{pmatrix}^T$; $v_s = \begin{pmatrix} v_{sd} & v_{sq} \end{pmatrix}^T$; $v_r = \begin{pmatrix} v_{rd} & v_{rq} \end{pmatrix}^T$; $y_r = i_r = \begin{pmatrix} i_{rd} & i_{rq} \end{pmatrix}^T$;

$$A_{rc}(\omega) = \begin{pmatrix} -\left(\frac{a+1}{T_r} + \frac{a}{T_s}\right) & \omega_s - \omega & \frac{a}{L_m T_s} & -\frac{a\omega}{L_m} \\ \omega - \omega_s & -\left(\frac{a+1}{T_r} + \frac{a}{T_s}\right) & \frac{a\omega}{L_m} & \frac{a}{L_m T_s} \\ \frac{L_m}{T_s} & 0 & -\frac{1}{T_s} & \omega_s \\ 0 & \frac{L_m}{T_s} & -\omega_s & -\frac{1}{T_s} \end{pmatrix};$$

$$B_s = \begin{pmatrix} -\frac{1-\sigma}{\sigma L_m} & 0 \\ 0 & -\frac{1-\sigma}{\sigma L_m} \\ 1 & 0 \\ 0 & 1 \end{pmatrix}; \quad B_r = \begin{pmatrix} \frac{1}{\sigma L_r} & 0 \\ 0 & \frac{1}{\sigma L_r} \\ 0 & 0 \\ 0 & 0 \end{pmatrix}; \quad C_{rc} = \begin{pmatrix} 1 & 0 & 0 & 0 \\ 0 & 1 & 0 & 0 \end{pmatrix};$$

$v_{sd}, v_{sq}, v_{rd}, v_{rq}, i_{sd}, i_{sq}, i_{rd}, i_{rq}$ are voltage and current components of the stator and rotor respectively; Ψ_{sd}, Ψ_{sq} are stator flux components; L_s, L_r are stator and rotor inductances; L_m is mutual inductance; R_s, R_r are stator and rotor resistances; $\sigma = 1 - \frac{L_m^2}{L_s L_r}$ is the total linkage coefficient; $a = \frac{1-\sigma}{\sigma}$; $T_s = \frac{L_s}{R_s}$ and $T_r = \frac{L_r}{R_s}$ denote the time constants of stator and rotor; $\omega = \omega_s - \omega_r$ is the mechanical angular velocity of the rotor; ω_s is electrical angular velocity of stator (or grid); and ω_r is electrical angular velocity of rotor.

In the literature, the classical approach to DFIM vector control [1] allows one to achieve decoupled control of active and reactive power in both generator and motor operations. The control structure of DFIM including PI current controllers is described in [2, 3, 4, 5]. In some cases, the cross coupling term in the rotor equations that includes the mechanical angular speed is eliminated by adding a feed-forward term to the output of the q-axis controller [3, 6]. In these cases the difficulties of the nonlinear dynamics of the doubly-fed induction generator (DFIG) are not taken into account, i.e., the model of the machine is linearized and it is assumed that both the machine parameters required by the control algorithm and the grid voltage are precisely known. Clearly, such controller designs might result in a closed-loop behavior that is highly sensitive to a change in operating conditions and/or parameters.

In order to improve the system performance against changes in the machine parameters and exogenous inputs, an H_∞ control approach for an induction generator in windmill power system is proposed in [7] and for induction motor control in [8]. Recently, the LPV current control approach, which takes the parameter variations into account directly in the control design, is applied for an induction motor in [9, 10]. In [10], the electrical angular rotor speed and the estimated magnetizing current are considered to be varying parameters. The control objective is to track references for the magnetizing current and the angular electrical rotor speed. A quasi-LPV approach is applied to the design of a stator current controller and a speed controller. In [9], the same method is employed for the inner current control loop, and the LPV controller synthesis is extended to a discrete time setting.

Our paper presents an alternative control strategy for DFIMs. The control objective is to track references for the electrical torque and the power factor. The mechanical angular speed ω in (1) is considered as a time-varying parameter. This particular choice is motivated by the fact that ω, which causes the system to be nonlinear, can be measured online. Actually, its value varies by $\pm 30\%$ around the synchronous

speed ω_s. Therefore, with $-1 \le \delta_\omega \le 1$ and $p_\omega = 0.3$, the mechanical angular speed can be expressed as $\omega = \omega_s(1 + p_\omega \delta_\omega)$. Thus (1) now becomes affinely parameter dependent and can be rewritten as

$$\dot{x}_r = (A_{rs} + \delta_\omega A_{r\omega})x_r + B_s v_s + B_r v_r \tag{3}$$

where $A_{rs}, A_{r\omega}$ are time-invariant matrices defined by

$$A_{rs} = \begin{pmatrix} -\left(\frac{a+1}{T_r} + \frac{a}{T_s}\right) & 0 & \frac{a}{L_m T_s} & -\frac{a\omega_s}{L_m} \\ 0 & -\left(\frac{a+1}{T_r} + \frac{a}{T_s}\right) & \frac{a\omega_s}{L_m} & \frac{a}{L_m T_s} \\ \frac{L_m}{T_s} & 0 & -\frac{1}{T_s} & \omega_s \\ 0 & \frac{L_m}{T_s} & -\omega_s & -\frac{1}{T_s} \end{pmatrix}; \quad A_{r\omega} = \begin{pmatrix} 0 & -\omega_s p_\omega & 0 & -\frac{a\omega_s p_\omega}{L_m} \\ \omega_s p_\omega & 0 & \frac{a\omega_s p_\omega}{L_m} & 0 \\ 0 & 0 & 0 & 0 \\ 0 & 0 & 0 & 0 \end{pmatrix}.$$

Since the system is affinely parameter dependent, this paper is mainly concerned with synthesizing an affine parameter-dependent controller.

1.2 Rotor side controllers

Besides transferring active and reactive powers between the rotor and the grid, the grid side controller has to maintain the DC-link voltage at a constant value, while the rotor side controller is aimed to control active and reactive powers by regulating the electrical torque T_e and the power factor φ_g.
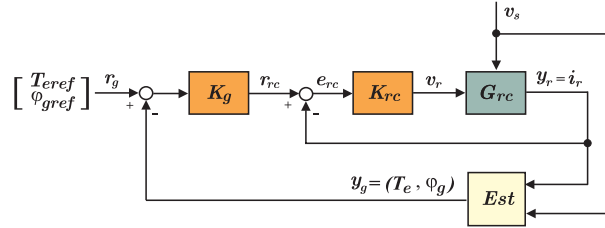

Figure 2: Rotor side current control loop

The control structure on the rotor side of DFIM has two loops. The inner loop with controller K_{rc} is called rotor current control loop. The controller design goal of the rotor current controller K_{rc} is to have high dynamic performance and robust tracking of the rotor currents. The outer loop with controller K_g is called electrical torque control loop used for tracking optimal values of electrical torque T_e^{ref} and power factor φ_g^{ref}. In Figure 2, G_r represents the plant corresponding to equations (1) and (2); y_g is the controlled output that is estimated from the outputs of the plant. Based on the actual measured values of the wind speeds and the characteristics of each particular wind turbine, the main control station will track the optimum torque from a look-up table and use it as the reference value for the power electronics control stage.

The electrical torque of the DFIM on the dq reference frame aligned to the stator voltage, $\Psi_{sd} = 0$, can be computed by

$$T_e = -\frac{3}{2} p \frac{L_m}{L_s} \Psi_{sq} i_{rd}. \tag{4}$$

On the other hand, controlling the reactive power can be implemented by regulating the power factor φ. This factor can be computed as follows

$$\varphi = arcsin \frac{i_{sq}}{\sqrt{i_{sd}^2 + i_{sq}^2}}. \tag{5}$$

The equations (4), and (5) show that the variables of torque and power factor of DFIM can be regulated via the components of the rotor currents i_{rd} and i_{rq}.

2 LPV controller synthesis for affinely parameter-dependent systems

2.1 $\mathcal{L}_2$-gain performance

Let us consider an LPV system that is described as

$$
\left(\begin{array}{c} \dot{x}(t) \\ \hline z_p(t) \\ y(t) \end{array}\right) = \left(\begin{array}{c|cc} A(\delta(t)) & B_p(\delta(t)) & B(\delta(t)) \\ \hline C_p(\delta(t)) & D_p(\delta(t)) & E(\delta(t)) \\ C(\delta(t)) & F(\delta(t)) & 0 \end{array}\right) \left(\begin{array}{c} x(t) \\ \hline w_p(t) \\ u(t) \end{array}\right)
\tag{6}
$$

where the matrices in (6) are affine functions of the parameter vector that varies in the polytope δ_c with vertices $\delta^1,...,\delta^k$, that is

$$
\delta(t) \in \delta_c = conv\left\{\delta^1,...,\delta^k\right\} \triangleq \left\{\sum_{j=1}^{k}\lambda_j\delta^j, \quad \lambda_j \geq 0, \quad \sum_{j=1}^{k}\lambda_j = 1\right\}
\tag{7}
$$

The optimization problem is to search for an LPV controller that is defined with affine functions as

$$
\left(\begin{array}{c} \dot{x}_c(t) \\ u(t) \end{array}\right) = \left(\begin{array}{cc} A_c(\delta(t)) & B_c(\delta(t)) \\ C_c(\delta(t)) & D_c(\delta(t)) \end{array}\right) \left(\begin{array}{c} x_c(t) \\ y(t) \end{array}\right)
\tag{8}
$$

such that the closed-loop system of (6) and (8)

$$
\left(\begin{array}{c} \dot{\xi}(t) \\ z_p(t) \end{array}\right) = \left(\begin{array}{cc} \mathcal{A}(\delta(t)) & \mathcal{B}(\delta(t)) \\ \mathcal{C}(\delta(t)) & \mathcal{D}(\delta(t)) \end{array}\right) \left(\begin{array}{c} \xi(t) \\ w_p(t) \end{array}\right)
\tag{9}
$$

is internally stable and the L_2-norm of $w_p(t) \to z_p(t)$ is bounded by a given number $\gamma > 0$ for all possible parameter trajectories $\delta : [0,\infty) \to \delta_c$.

Note that the matrices $\mathcal{A}(\cdot)$, $\mathcal{B}(\cdot)$, $\mathcal{C}(\cdot)$, and $\mathcal{D}(\cdot)$ in (9) are given as

$$
\left(\begin{array}{c|c} \mathcal{A}(\delta(t)) & \mathcal{B}(\delta(t)) \\ \hline \mathcal{C}(\delta(t)) & \mathcal{D}(\delta(t)) \end{array}\right) =
$$
$$
\left(\begin{array}{cc|c} A(\delta(t))+B(\delta(t))D_c(\delta(t))C(\delta(t)) & B(\delta(t))C_c(\delta(t)) & B_p(\delta(t))+B(\delta(t))D_c(\delta(t))F(\delta(t)) \\ B_c(\delta(t))C(\delta(t)) & A_c(\delta(t)) & B_c(\delta(t))F(\delta(t)) \\ \hline C_p(\delta(t))+E(\delta(t))D_c(\delta(t))C(\delta(t)) & E(\delta(t))C_c(\delta(t)) & D_p(\delta(t))+E(\delta(t))D_c(\delta(t))F(\delta(t)) \end{array}\right).
$$

The characterization of robust stability and performance for the closed-loop system (9) is provided by the following theorem:

Theorem 2.1 *If there exists a constant matrix $X \succ 0$ for which*

$$
\left(\begin{array}{cc} I & 0 \\ \mathcal{A}(\delta) & \mathcal{B}(\delta) \\ \hline 0 & I \\ \mathcal{C}(\delta) & \mathcal{D}(\delta) \end{array}\right)^T \left(\begin{array}{cc|cc} 0 & X & 0 & 0 \\ X & 0 & 0 & 0 \\ \hline 0 & 0 & -\gamma I & 0 \\ 0 & 0 & 0 & \frac{1}{\gamma}I \end{array}\right) \left(\begin{array}{cc} I & 0 \\ \mathcal{A}(\delta) & \mathcal{B}(\delta) \\ \hline 0 & I \\ \mathcal{C}(\delta) & \mathcal{D}(\delta) \end{array}\right) \prec 0 \quad \text{holds for all } \delta \in \delta_c,
\tag{10}
$$

then the system (9) is uniformly exponentially stable and the L_2 gain from w_p to z_p is bounded by γ. $\square$

Proof: See [11].

Since the system (6) is affinely parameter-dependent with respect to the time-varying parameter $\delta(t)$ in (7), the state-space matrices of (6) range in the polytope defined as follows [12]:

$$
\left(\begin{array}{ccc} A(\delta(t)) & B_p(\delta(t)) & B(\delta(t)) \\ C_p(\delta(t)) & D_p(\delta(t)) & E(\delta(t)) \\ C(\delta(t)) & F(\delta(t)) & 0 \end{array}\right) \in conv\left\{\left(\begin{array}{ccc} A^j & B_p^j & B^j \\ C_p^j & D_p^j & E^j \\ C^j & F^j & 0 \end{array}\right)\right.
$$
$$
\triangleq \left.\left(\begin{array}{ccc} A(\delta^j) & B_p(\delta^j) & B(\delta^j) \\ C_p(\delta^j) & D_p(\delta^j) & E(\delta^j) \\ C(\delta^j) & F(\delta^j) & 0 \end{array}\right), j = 1,...,k\right\}.
$$

If $\begin{pmatrix} B \\ E \end{pmatrix}$ and $\begin{pmatrix} C & F \end{pmatrix}$ are parameter independent, the describing matrices for the closed-loop system (9) are also affine in the parameter, i.e.

$$\begin{pmatrix} \mathcal{A}(\delta(t)) & \mathcal{B}(\delta(t)) \\ C(\delta(t)) & \mathcal{D}(\delta(t)) \end{pmatrix} \in \mathrm{conv}\left\{ \begin{pmatrix} \mathcal{A}^j & \mathcal{B}^j \\ C^j & \mathcal{D}^j \end{pmatrix} \triangleq \begin{pmatrix} \mathcal{A}(\delta^j) & \mathcal{B}(\delta^j) \\ C(\delta^j) & \mathcal{D}(\delta^j) \end{pmatrix}, j = 1,...,k \right\}.$$

This implies for the synthesis inequalities (10) that we can replace the search over the polytope δ_c without loss of generality by the search over the extreme points $\delta^1,...,\delta^k$ of this set. Consequently, condition (10) can be reduced to a finite set of Linear Matrix Inequalities (LMIs) since it is equivalent to

$$\begin{pmatrix} I & 0 \\ \mathcal{A}(\delta^j) & \mathcal{B}(\delta^j) \\ \hline 0 & I \\ C(\delta^j) & \mathcal{D}(\delta^j) \end{pmatrix}^T \begin{pmatrix} 0 & X & 0 & 0 \\ X & 0 & 0 & 0 \\ \hline 0 & 0 & -\gamma I & 0 \\ 0 & 0 & 0 & \frac{1}{\gamma}I \end{pmatrix} \begin{pmatrix} I & 0 \\ \mathcal{A}(\delta^j) & \mathcal{B}(\delta^j) \\ \hline 0 & I \\ C(\delta^j) & \mathcal{D}(\delta^j) \end{pmatrix} \prec 0 \quad \text{for all } j = 1,..,k. \tag{11}$$

2.2 LPV controller synthesis

Elimination of the controller parameters in (11) leads to the following LMI conditions that guarantee the existence of a polytopic LPV controller [12, 13, 14]:

$$\begin{pmatrix} Y & I \\ I & X \end{pmatrix} \succ 0 \tag{12}$$

$$\Phi_x^T \begin{pmatrix} XA(\delta^j) + A(\delta^j)^T X & XB_p(\delta^j) & C_p(\delta^j)^T \\ B_p(\delta^j)^T X & -\gamma I & D_p(\delta^j)^T \\ C_p(\delta^j) & D_p(\delta^j) & -\gamma I \end{pmatrix} \Phi_x \prec 0 \tag{13}$$

$$\Phi_y^T \begin{pmatrix} A(\delta^j)Y + A(\delta^j)^T Y & B_p(\delta^j) & YC_p(\delta^j)^T \\ B_p(\delta^j)^T & -\gamma I & D_p(\delta^j)^T \\ C_p(\delta^j)Y & D_p(\delta^j) & -\gamma I \end{pmatrix} \Phi_y \prec 0 \tag{14}$$

for $j = 1,..,k$, where Φ_x and Φ_y form bases for $ker\begin{pmatrix} B^T & 0 & E^T \end{pmatrix}$ and $ker\begin{pmatrix} C & F & 0 \end{pmatrix}$ respectively.

After obtaining X and Y over the constraint LMIs (12)-(14), the controller parameters at each δ^j can be reconstructed by using the projection lemma [11]. Then a vertex controller K_j is any solution that satisfies (11) for the corresponding index j.

Finally, the controller is implemented as follows: at time t we determine coefficients $\lambda_1(t),...,\lambda_k(t)$ which represent $\delta(t)$ according to (7), and we use

$$K(t) \triangleq \sum_{j=1}^{k} \lambda_j(t) K_j = \sum_{j=1}^{k} \lambda_j(t) \begin{pmatrix} A_{kj} & B_{kj} \\ C_{kj} & D_{kj} \end{pmatrix} \tag{15}$$

as the system matrix for simulation.

3 Gain-scheduling design for the rotor side current controller

3.1 System representation when the rotor angular speed ω is treated as an uncertainty

With $\Delta_\omega = \begin{pmatrix} \delta_\omega & 0 \\ 0 & \delta_\omega \end{pmatrix}$, the system (3) can be rewritten as follows:

$$\begin{pmatrix} \dot{x}_r \\ \hline y_r \\ z_\omega \end{pmatrix} = G_{rc} \begin{pmatrix} x_r \\ v_s \\ \hline v_r \\ w_\omega \end{pmatrix}, \quad w_\omega = \Delta_\omega z_\omega \tag{16}$$

where

$$G_{rc} = \begin{pmatrix} A_{rs} & B_s & B_r & B_{r\omega} \\ \hline C_{rc} & 0 & 0 & 0 \\ C_{r\omega} & 0 & 0 & 0 \end{pmatrix};$$

$$C_{r\omega} = \begin{pmatrix} 0 & -\omega_s p_\omega & 0 & -\frac{a\omega_s p_\omega}{L_m} \\ \omega_s p_\omega & 0 & \frac{a\omega_s p_\omega}{L_m} & 0 \end{pmatrix}; \quad B_{r\omega} = \begin{pmatrix} 1 & 0 & 0 & 0 \\ 0 & 1 & 0 & 0 \end{pmatrix}^T; \quad y_r = \begin{pmatrix} i_{rd} & i_{rq} \end{pmatrix}^T.$$

3.2 H_∞ control of the LPV system

A mixed sensitivity T/S loop shaping H_∞ optimization is proposed for the rotor current control loop (see Figure 2). The external control inputs w_{rc} consist of stator voltages and reference rotor currents $w_{rc} = \left(v_{sd} \quad v_{sq} \quad i_{rd}^{ref} \quad i_{rq}^{ref} \right)^T$. The controller outputs are $v_r = \left(v_{rd} \quad v_{rq} \right)^T$. The controller inputs or tracking errors are $e_r = \left(e_{rcd} \quad e_{rcq} \right)^T = \left(i_{rd}^{ref} - i_{rd} \quad i_{rq}^{ref} - i_{rq} \right)^T$. The measured outputs are $y_r = \left(i_{rd} \quad i_{rq} \right)^T$. The sensitivity function is $S_{rc} = (I + G_{rc}K_{rc})^{-1}$ and the complementary sensitivity function is $T_{rc} \overset{\Delta}{=} I - S_{rc}$. The interconnection of the system is shown in Figure 3. The weighting function $W_{rs} = \begin{pmatrix} W_{rsd} & 0 \\ 0 & W_{rsq} \end{pmatrix}$ is a first-order low-pass filter used to shape the sensitivity for tracking. The weighting function $W_{rt} = \begin{pmatrix} W_{rtd} & 0 \\ 0 & W_{rtq} \end{pmatrix}$ is a first-order high-pass filter used to shape the complementary sensitivity function to guarantee the robustness against high frequency un-modelled dynamics.
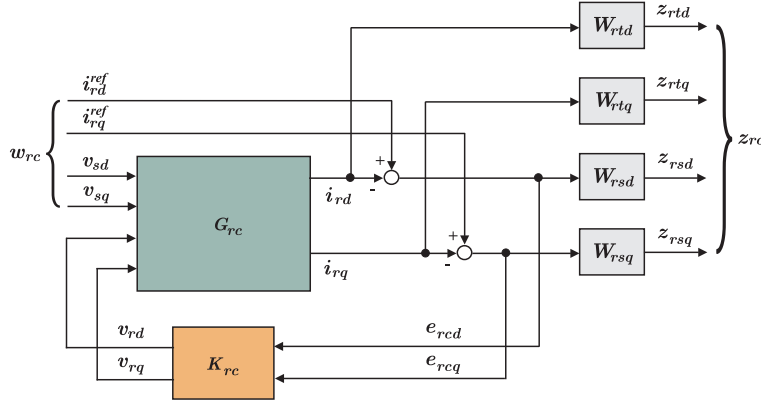

Figure 3: The interconnection of the system

The standard H_∞ control problem is to find a stabilizing LTI controller $K_{rc}(\omega)$ at fixed frozen values of ω such that the H_∞-norm of the channel $w_{rc} \to z_{rc}$ is smaller than a given number γ.

3.3   Synthesis of gain-scheduled current controller

The gain-scheduled controller synthesis is similar to the classical H_∞ synthesis, but both the plant and the controller are now LPV systems. The optimization problem is to find a stabilizing controller $K_{rc}(\omega)$ such that the $\mathcal{L}_2$-gain of the channel $w_{rc} \to z_{rc}$ is smaller than γ for all trajectories of $\omega(t) \in [\omega_{min}, \omega_{max}] = [(1 - p_\omega)\omega_s, (1 + p_\omega)\omega_s]$.

The synthesis LMIs (12)-(14) are solved by using the LMI Control Toolbox [15]. If a solution (X, Y) is given, the vertex controllers K_j are constructed as solutions of (11). Now we are ready to compute the polytopic LPV controller by measuring values of ω online and by getting a vertex decomposition as expressed in (7). Then the state-space matrices describing the LPV controller are also given online by the interpolation

$$\begin{pmatrix} A_{Krc}(t) & B_{Krc}(t) \\ C_{Krc}(t) & D_{Krc}(t) \end{pmatrix} = \frac{\delta_w^{max} - p(t)}{\delta_w^{max} - \delta_w^{min}} \begin{pmatrix} A_{Krc1} & B_{Krc1} \\ C_{Krc1} & D_{Krc1} \end{pmatrix} + \frac{p(t) - \delta_w^{min}}{\delta_w^{max} - \delta_w^{min}} \begin{pmatrix} A_{Krc2} & B_{Krc2} \\ C_{Krc2} & D_{Krc2} \end{pmatrix}$$

where $p(t) = \frac{\omega(t) - \omega_s}{\omega_s p_w}$.

4 Simulations

4.1 Performance of the system with dynamic wind

When the wind speed is less than the rated wind speed, the objective is to maximize the captured energy by adjusting the rotor speed in order to operate the turbine along the maximum power curve or, in other words, to keep the tip-speed ratio optimal. As the wind speed increases, the generator is allowed to accelerate until it reaches its rated speed. The pitch angle values in the power optimization region are all found close to zero for the given wind turbine. When the wind speed is higher than the rated wind speed, the input power from the generator is maintained at its rated power by increasing the pitch angle to keep the electrical power output at rated power. Hence, the pitch angle control is mostly used above rated wind speed to prevent overload of the generator power. The performances of the controlled system with the LPV controller under wind speed changes is shown in figure 4.
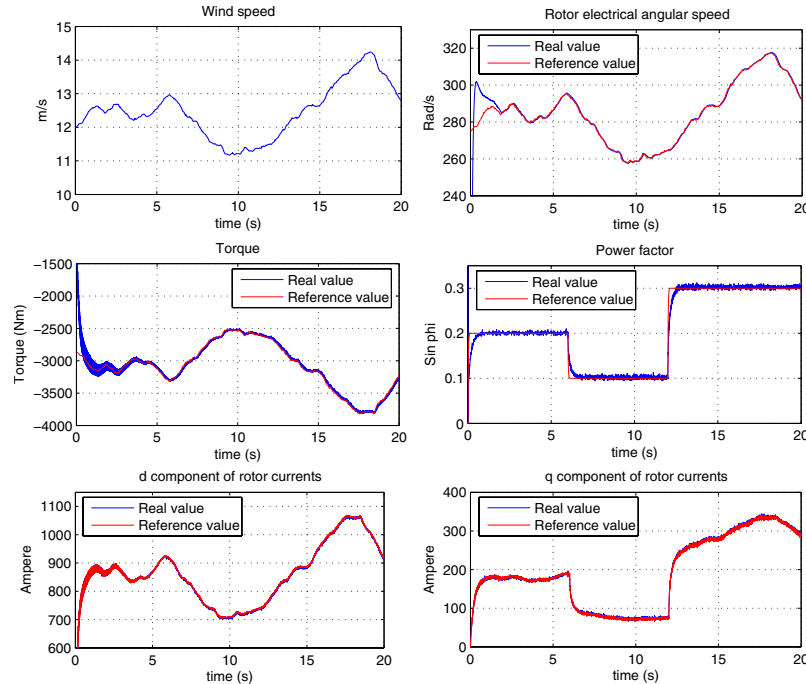

Figure 4: The performance of the system with dynamic wind

4.2 Performance comparison of deadbeat and LPV controllers

In this study two complete simulation models, one based on a conventional control scheme that is called dead-beat control (similar to that in [16]) and the other based on the described LPV framework are developed for the control of the electrical torque and the power factor on the rotor side in order to compare the performance of the closed loop systems.

4.2.1 Performance of the system with step changes

Figure 5 shows the performance of the system tested with step changes of the set-point values of i_{rd} and i_{rq}. From 0 to 0.05s the stator windings are open. The stator voltages are regulated so as to be equivalent to grid voltages in amplitude and phase. After that, the stator windings are connected to the grid and the transient period appears to be about 0.2s. At the beginning of the transient period, the rotor currents may fluctuate strongly due to sudden increase of stator flux and currents. The simulation results show that the variations of the rotor currents during the transient period with the LPV controller are much smaller than those for the deadbeat controller.
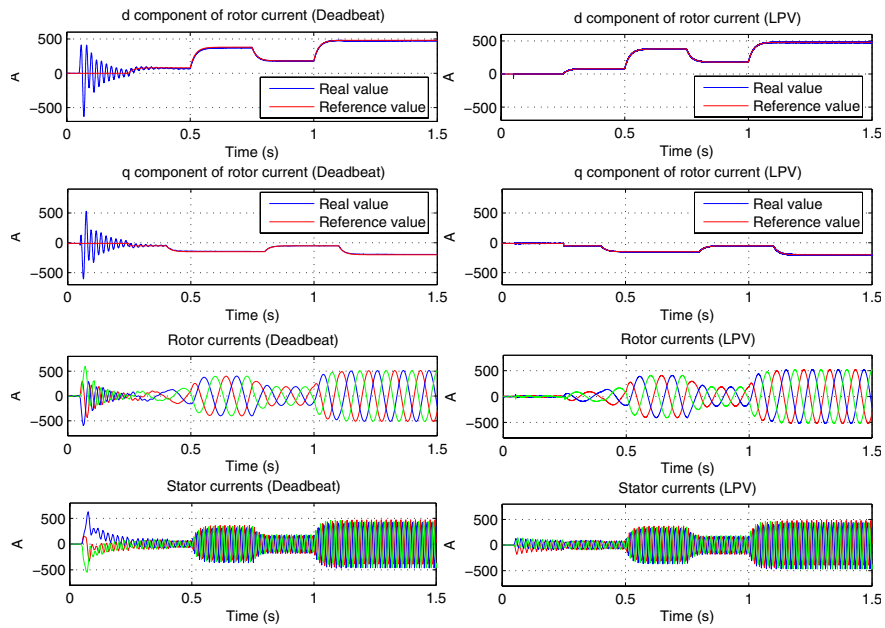
Figure 5: Transient period of voltages and currents with gird synchronization (left: dead-beat controller, right: self-scheduled controller)

4.2.2 Robustness of the control system against other parameter changes

By varying the values of L_s we see form Figure 6 that the system with dead-beat controller stays stable if the L_s deviates by $[97.9\%, 101.12\%]$ of its nominal values, while with the self-scheduled controller this range is $[95.8\%, 150\%]$.

Similarly, by varying the values of L_r we see from Figure 7 that the system with dead-beat controller stays stable if the L_r deviates by $[97.84\%, 125\%]$ from its nominal value, while with the self-scheduled controller this range is $[95.68\%, 150\%]$.
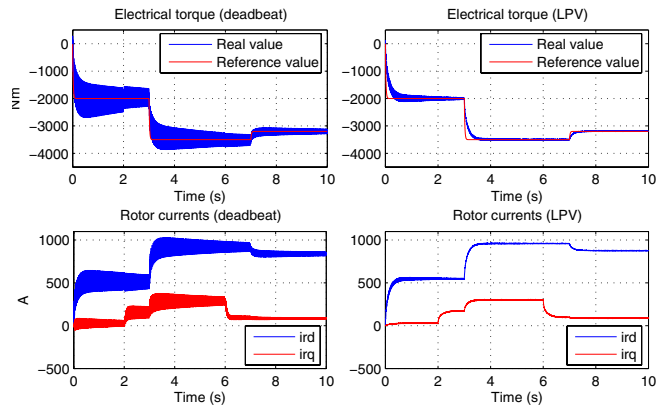

Figure 6: L_s decreases to 2.1% of the normal value (left: dead-beat controller, right: self-scheduled controller)

4.2.3 The impact of stator voltage dips on the robustness of the control system

When the grid undergoes a fault, the sag in the grid voltage will result in an increase of the current in the stator windings of the DFIM. Because of the magnetic coupling between stator and rotor, this current will also flow into the rotor circuit and the power converter leading to the destruction of the converter if nothing is done to protect it. On the other hand, the study in [5] shows that the dynamics of the DFIM has
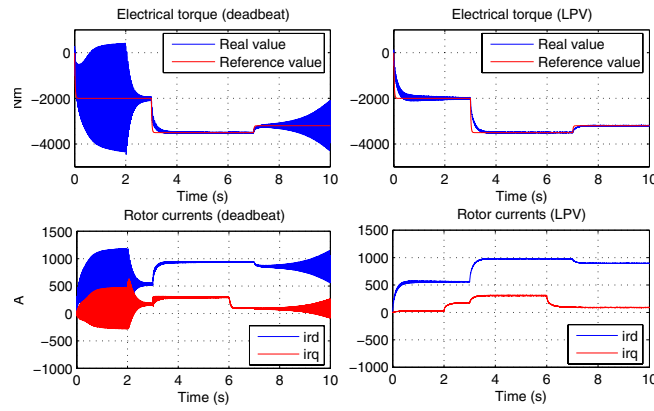
Figure 7: L_r decreases to 2.16% of the normal value (left: dead-beat controller, right: self-scheduled controller)

poorly damped poles in the transfer function of an LTI model of the machine. This will cause oscillations in the flux if the DFIM is affected by grid disturbances. After such disturbances, an increased rotor voltage will be needed to control the rotor currents. When this required voltage exceeds the voltage limit of the converter, it is not possible any longer to control the current as desired [17]. Therefore, the control system should maintain operation and reduce oscillations as much as possible during grid voltage faults. A comparison of the performance between the dead-beat control and the scheduled control systems in
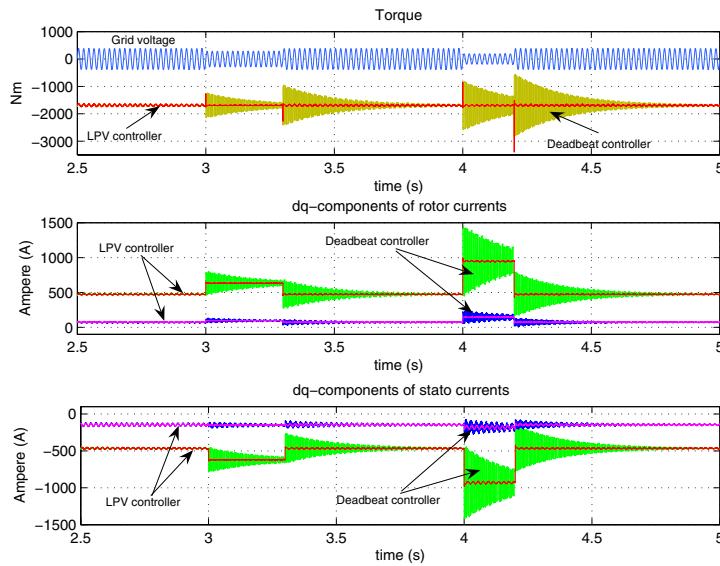

Figure 8: The performance of the system when grid voltage is faulty

the presence of grid voltage faults is presented in Figure 8. The grid voltage was dropped down to 25% of the normal voltage. This phenomenon occurred in a period of 300 msec before it recovered to its rated value. After that, the grid voltage once again was dropped to 50% of the rated voltage during 200 msec. The graphs show that the oscillations of torque and currents in the case of self-scheduled control were remarkably dampened at the grid voltage fault time.

5   Conclusion

The self-scheduled LPV control method has been applied to design the rotor side current controller for the DFIM in a variable speed wind turbine system, where the online measurable rotor mechanical

angular speed is considered as the time varying parameter. Hence the designed controller maintains the performance requirements for all trajectories of rotor speed over its variation range in a systematic way. A classical control approach, the so-called dead-beat controller, is also developed for the control of the electrical torque and the power factor on the rotor side. Under disadvantageous variations of machine parameters and for grid voltage dips, simulation results show that the designed LPV controller is far more robust than the dead-beat controller. Oscillations in the stator and rotor currents are considerably reduced during the grid voltage faults, and the closed loop system recovers from the faults much faster than in the conventional case. Hence, the new control scheme improves the performance of the closed-loop DFIM considerably.

Experiments on a real-time laboratory set up are currently performed, and a more thorough analysis of the performance improvements are being investigated.

References

[1] W. Leonhard. *Control of electrical drives*. Springer, 1996.

[2] A. Tapia, G. Tapia, and J. X. Ostolaza. Reactive power control of wind farms for voltage control applications. *Renewable Energy*, 29:377–392, 2004.

[3] B. Hopfensperger, D.J. Atkinson, and R. A. Lakin. Stator flux oriented control of a double-fed induction machine with and without position encoder. *IEE Proc.-Electr. Power Appl.*, 147:241–250, 2000.

[4] R. Pena, J. C. Clare, and G. M. Asher. Doubly fed induction generator using back-to-back pwm converters and its application to variable speed windenergy generator. *IEE Proceedings on Electric Power Applications*, 143:231–241, 1996.

[5] A. Petersson. *Analysis, Modeling and Control of Doubly-Fed Induction Generators for Wind Turbines*. PhD thesis, Chalmers University of Technology, 2003.

[6] A. Petersson, L. Harnefors, and T. Thiringer. Evaluation of current control methods for wind turbines using doubly fed induction machines. *IEEE transactions on Power Electronics*, 20:227–235, 2005.

[7] Y. Long, H. Miyagi, and K. Yamashita. Windmill power systems controller design using H_∞ theory. *IEEE International Conference on Systems, Man, and Cybernetics*, 5:3490–3495, 2000.

[8] A. Makouf, M. E. H. Benbouzid, D. Diallo, and N. E. Bouguechal. Induction motor robust control: an H_∞ control approach with field orientation and input-output linearizing. *The 17th annual conference of the IEEE industrial electronics society*, 2:1406 – 1411, 2001.

[9] J.D. Bendtsen and K. Trangbaek. Discrete-time LPV current control of an induction motor. *IEEE Conference on Decision and Control*, 6:5903– 5908, Dec 2003.

[10] K. Trangbek. *Linear Parameter Varying Control of Induction Motors*. PhD thesis, Aalborg University, Denmark, 2001.

[11] C. Scherer and S. Weiland. *Linear Matrix Inequalities in Control*. Lecture notes in DISC course, 2005.

[12] P. Apkarian, P. Gahinet, and G. Becker. Self-scheduled H_∞ control of linear parameter varying systems: a design example. *Automatica*, 31:1251–1261, 1995.

[13] S. Bennani, D. M. C. Willemsen, and C. W. Scherer. Robust LPV control with bounded parameter rates. *AIAA Guidance, Navigation, and Control Conference, New Orleans, LA*, pages 1080–1089, Aug. 11-13, 1997.

[14] P. Apkarian and R.J. Adams. Advanced gain-scheduling techniques for uncertain systems. *IEEE Transactions on Control Systems Technology*, 6:21 – 32, Jan. 1998.

[15] P. Gahinet, A. Nemirovski, A. J. Laub, and M. Chilali. *LMI Control Toolbox for use with Matlab*, volume 1. The Mathworks, 1995.

[16] N. P. Quang, A. Dittrich, and A. Thieme. Doubly-fed induction machine as generator: control algorithms with decoupling of torque and power factor. *Electrical Engineering (Archiv fur Elektrotechnik)*, 80:325–335, 1997.

[17] M. Johan and S. W. H. de Haan. Ridethrough of wind turbines with doubly-fed induction generator during a voltage dip. *IEEE Transactions on energy conversion*, 20:435–441, Jun 2005.